THE HIGH-MAGNESIUM CALCITE ORIGIN OF NUMMULITID FORAMINIFERA AND IMPLICATIONS FOR THE IDENTIFICATION OF CALCITE DIAGENESIS

LAURA J. COTTON[1*], DAVID EVANS[2], AND SIMON J. BEAVINGTON-PENNEY[3]

[1] *School of Earth and Ocean Sciences, Main Building, Park Place, Cardiff, CF10 3YE, UK*

Current address: School of Environment, Geography and Geosciences, University of Portsmouth, Burnaby building, Burnaby Road, Portsmouth, UK

[2] *Institute of Geosciences, Goethe University Frankfurt, 60438 Frankfurt am Main, Germany*

[3] *The University of Manchester, Williamson Building, Oxford Road, Manchester, M13 9PL*

email: laura.cotton@port.ac.uk

Abstract

Nummulites **were one of the most abundant and widespread larger benthic foraminifera of the Paleogene, however, confusion remains as to whether their original test mineralogy was high or low magnesium calcite within the literature. As studies using proxies based on** ***Nummulites*** **and related nummulitid geochemistry increase, it is essential to have a good understanding of test composition to assess preservation within potential samples, and to interpret results. Here we employ a combination of X-ray diffraction, Fourier transform infra-red spectroscopy and laser ablation ICPMS to determine magnesium content across exceptionally preserved and poorly preserved fossil material as well as modern examples of nummulitids, showing conclusively a primary intermediate to high magnesium calcite**

composition. This composition appears to be closely related to fluctuating ocean chemistry through the Paleogene. Using these results as an indicator of preservation we examine variation in trace element data across a suite of samples, and introduce the concept of the preservagram, a method of quickly visualising different styles of carbonate diagenesis.

INTRODUCTION

The Nummulitidae are one of the most long-ranging, widespread and abundant larger benthic foraminiferal families of the Cenozoic. This family includes not only the well-known genus *Nummulites* but also related forms including, among others, *Operculina*, *Heterostegina* and *Cycloclypeus* (Blondeau, 1972). Within the Eocene, *Nummulites* are known to have reached exceptionally large sizes (up to 15 cm in diameter; Beavington-Penney and Racey (2004)) and occurred in rock-forming quantities throughout the shallow carbonate platforms of the Tethys, including several major oil bearing deposits in the North Africa (Racey 2001). *Nummulites* and nummulitids have been used extensively within biostratigraphy and evolutionary studies (e.g. Schaub 1981; Papazzoni 1998; Serra-Kiel et al. 1998; Less et al. 2008; Cotton and Pearson 2011; Papazzoni et al. 2017; Benedetti et al. 2018) but also increasingly in geochemical studies (e.g. Wefer and Berger 1980; Purton and Brasier 1999; Evans et al. 2013; Evans et al. 2018). Despite their abundance in the fossil record and frequent use, opinion on the original mineralogy of *Nummulites* and nummulitids remains divided, with authors quoting both high magnesium (HMC typically 11-19 mole% $MgCO_3$; e.g. Bathurst 1976; Macauley et al 2001; Whittle and Alsharhan 1994) and low magnesium calcite (LMC; 1-4% $MgCO_3$) compositions (e.g. Hallock et al. 1991; Sen Gupta 1999; Debebay et al. 2000; Hohenegger et al. 2000) for fossil material.

45 Establishing the primary mineralogy of the nummulitids, and of widely utilised fossils in
46 general, is important as it provides a method with which to determine specimens with
47 exceptional preservation. This enables material that is sufficiently well-preserved to reliably
48 record primary geochemical information to be identified. A number of recent studies have aimed
49 to identify geochemical fingerprints of diagenesis and contamination, which may occur at a sub-
50 micron scale even when samples are visually well-preserved. For example, Sr/Ca ratios have
51 been used to identify selective dissolution (Stoll et al. 1999), elevated Mn/Ca may be indicative
52 of overgrowths (Pena 2005; Creech et al. 2010), and clay mineral contamination may result in
53 elevated Al/Ca. Therefore, understanding not only the primary mineralogy, but also the primary
54 geochemical composition of fossil material is a useful means of assessing the integrity of
55 geochemical datasets by providing a baseline to which samples can be compared.
56 A number of authors have noted that living and fossil perforate hyaline foraminifera – a
57 group which includes the nummulitids, are predominantly composed of LMC (Hallock et al.
58 1991; Sen Gupta 1999; Debebay et al. 2000; Hohenegger et al. 2000; Holail 1994; James et al.
59 1999). However, Blackmon and Todd (1959) showed that foraminifera with both LMC and
60 HMC tests are included within the radial hyaline "group", whilst Chave (1964) and Brenchley
61 and Harper (1998) observed most shallow benthic foraminifera were HMC. A number of authors
62 have also concluded the Paleogene genus *Nummulites* was originally HMC (Bathurst 1976;
63 Macauley et al. 2001; Whittle and Alsharhan 1994) and Milliman (1974) noted the extant
64 nummulitid *Heterostegina* is composed of HMC. Dolomitization and diagenesis of *Nummulites*-
65 rich carbonate deposits has also been used as an additional method of inferring original test
66 mineralogy. For example, the Rus formation, Abu Dhabi, United Arab Emirates is a heavily

dolomitised, shallow water limestone deposit, comprised largely of *Nummulites* along with other LBF and echinoderm fragments (Whittle and Alsharhan 1994). Whittle and Alsharhan (1994) suggest that the dolomitisation of the formation occurred due to a combination of meteoric mixing and the recrystallisation of a high proportion of originally HMC components (*Nummulites* and echinoderm fragments) to LMC, although they did not analyse the composition of the *Nummulites* tests directly. The El Garia formation, Tunisia is a very similar deposit with localised dolomitisation within a *Nummulites*-rich limestone (Beavington-Penney et al. 2008). Macaulay et al. (2001) obtained $MgCO_3$ values of 0.5±0.1 mole% using X-ray diffraction, indicating a LMC composition, but sediments forming this deposit have been deeply buried and have undergone extensive recrystallisation (see Beavington-Penney et al. 2008). The transformation of the *Nummulites* tests from HMC to LMC during diagenesis was therefore proposed as the source of the Mg^{2+} ions required for later dolomitisation, despite the LMC values obtained from the *Nummulites* tests themselves. The nummulitic limestones of the Giza Pyramids Plateau also show dolomitisation, however Holail (1994) suggested that *Nummulites* was originally LMC and that seawater provided the Mg^{2+} necessary for dolomitisation to occur.

This uncertainty is largely due to the instability of HMC. High magnesium calcite readily reverts to low magnesium calcite during diagenesis meaning much fossil material will be LMC, even if it was originally HMC. As LBF almost exclusively inhabit shallow (< 100 m) warm, marine carbonate environments, and are therefore preserved within limestones, at least some degree of recrystalisation and/or replacement generally occurs during fossilisation. However, exceptional preservation of *Nummulites* preserved within clays has been demonstrated at a small number of sites, particularly the Kilwa district of Tanzania (Cotton and Pearson 2011)

89 and the South of the UK (Cotton et al. in press). We investigate the magnesium content of fossils
90 samples from these sites, along with examples showing visually average preservation and
91 modern specimens using X-ray diffraction, ATR-Fourier-transform infra-red spectroscopy and
92 laser ablation ICPMS. In addition, these results were used to examine how trace element ratios
93 frequently used to assess diagenetic alteration compare in known well-preserved and less well-
94 preserved samples. This enables us to assess whether site-specific diagenetic histories complicate
95 the use of e.g. Al/Ca, Mn/Ca, or Sr/Ca as independent markers of preservation in geochemical
96 studies, or whether, certain elemental ratios show threshold values that are always indicative of
97 recrystallisation.
98
99 ## MATERIAL AND METHODS
100 ### Fossil Material
101 Different species of the genus *Nummulites*, were analysed from four different Eocene localities:
102 Tanzania, Oman and two localities in the south of the UK. Echinoid fragments from the same
103 locality and sample in Tanzania were also analysed. The analytical techniques applied to each
104 sample are summarised in Table 1.
105 Tanzania: Site 11, 12 and 17 from the Tanzania Drilling Project have become world-renowned
106 for their exceptional preservation of calcareous microfossils, including the preservation of
107 aragonite (e.g. Bown et al. 2008; Pearson et al. 2008) and contain abundant LBF (Cotton and
108 Pearson 2012). Whilst the preservation of the LBF is variable, dependent on the lithology of
109 specific beds, many have the same exceptional preservation seen in the planktonic assemblages
110 (Evans et al. 2018). The succession is comprised of hemipelagic clays with occasional debris

111 flow limestone beds (Nicholas et al. 2006; Cotton and Pearson 2012), and spans the uppermost
112 Eocene to lowermost Oligocene (Pearson et al. 2008; Cotton and Pearson 2012). Glassy
113 specimens of *Nummulites* sp. 1 and *Nummulites* cf. *fabianii* (see Fig. 2 of Cotton and Pearson
114 (2011) for taxonomy) from five clay levels were analysed. LA-ICPMS analyses were performed
115 non-destructively on the marginal cord of 10 unbroken specimens. In order to collect XRD and
116 FTIR spectra, between one and three glassy, clay-level specimens were powdered with a pestle
117 and mortar for analysis; where specimens were combined the same species from the same core
118 level were used. Echinoderm test material from one of these levels was prepared for XRD and
119 FTIR in the same way as the *Nummulite*s as a comparison of a known HMC organism which
120 had undergone the same diagenetic history as the *Nummulites*. Under the microscope, the
121 specimen showed no evidence of infilling or overgrowths. A sample of *Nummulites cf. fabianii*,
122 from a poorly consolidated debris flow limestone and showing clear signs of infilling and
123 recrystallisation, was analysed for comparison.
124 Seeb formation, Oman: The Seeb formation of Oman is a middle Eocene limestone formed in a
125 carbonate ramp setting, and contains abundant *Nummulites ex. gr. perforatus* and *N. ex. gr.*
126 *gizehensis* (Racey, 1994, 1995; Beavington-Penney et al., 2006). The *Nummulites* tests show
127 generally poor to average preservation within a limestone, with some calcite infilling chambers,
128 but are not thought to have been deeply buried (Beavington-Penney et al., 2006). The specimens
129 used in the analysis were approximately 2 cm in diameter, therefore several samples taken on
130 different parts of the test (both inner and outer whorls) were used for XRD, whereas a single
131 specimen showing no obvious infilling in the equatorial chambers was crushed and homogenised
132 for FTIR. LA-ICPMS analysis was performed on the marginal cord of a sectioned specimen.

Alum Bay, UK: The lower most sediments of the Barton beds at Alum Bay on the Isle of Wight are located around the Lutetian- Bartonian transition (Cotton et al. 2020) and contain abundant *Nummulites prestwichianus*. Individuals occur in large numbers within a glauconitic clay, and often have a glassy surface to the test. Some specimens show evidence of infilling by pyrite, these were avoided in the study. Several specimens were combined to generate enough calcite for the XRD and FTIR analysis, LA-ICPMS analysis were performed on the marginal cord of sectioned specimens embedded in epoxy resin.

Bracklesham Group, UK: The Bracklesham beds are middle Eocene in age and contain abundant *Nummulites laevigatus*. The *Nummulites* at this locality are preserved in situ in glauconitic muds and are thought to be among the best preserved *Nummulites* in Europe (Curry et al. 1977; Purton and Brasier 1999). Specimens from beds E7 and E8 at this locality have been shown to preserve seasonal variation in stable isotopes (see Purton and Brasier 1999). Purton (1997) considered the preservation excellent with no secondary calcite evident in SEM and cathodoluminescence studies. The XRD and FTIR analysis was carried out on two specimens that, as typical of the locality, contained no infilling calcite. As for the Alum Bay samples, LA-ICPMS analyses were performed on the marginal cord of sectioned samples embedded in epoxy.

Modern Specimens

Operculina ammonoides, the nearest living relative of the Paleogene *Nummulites*, were hand-sampled from the Great Barrier Reef (GBR; 19.73°S, 150.22°E) from a water depth of 74 m (Renema et al. 2013; Evans et al. 2013). For LA-ICPMS analysis, multiple foraminifera were embedded in resin and ground down to expose the marginal cord.

155 *Cycloclypeus carpenteri*, a modern nummulitid, were collected from 77 m water depth offshore
156 Ishigaki Island (Japan) by J. Hohenegger (University of Vienna). The two XRD spectra of this
157 specimen were collected from a crushed specimens.
158
159 ## Analytical Techniques
160 ### *X-Ray Diffraction*
161 X-ray diffraction is a widely utilised crystallographic method of determining mineralogical
162 composition via lattice spacing. Within calcite, magnesium substitution decreases the lattice
163 spacing in the calcite crystal, which is measured by X-ray diffraction. Five curves relating the
164 shift of lattice spacing to mole% $MgCO_3$ have been proposed. Milliman (1974) suggests that the
165 graph of Goldsmith et al. (1961) is the most accurate. Matching the XRD data against this curve
166 gives an approximate Mg content of the lattice to within 0.5 mole%. Where necessary any shift
167 in the internal standard peak was used to calculate a correction factor for $d\theta$ values.
168 For X-ray diffraction analysis all samples were analysed using a PW1710 Philips automated
169 powder diffractometer (using a copper tube) run at 35kV 40 mA at Cardiff University, U.K.
170 Tests of specimens were washed in DI water to removed matrix, dried at room temperature or
171 within a low temperature oven (~30°), were crushed to a fine powder, mixed with KCl as an
172 internal standard and acetone added to form a paste. The paste was then pipetted and spread on a
173 glass slide. An internal standard is required as the exact location of the diffraction peak on the
174 recorder tracing depends on the thickness of paste and alignment of the X-ray generator, the
175 exact lattice spacing of the standard is known and can be used to correct any shift in the trace.
176

177 *Fourier transform infra-red spectronomy*

178 Fourier transform infra-red spectra were collected using a Bruker Platinum ATR infrared
179 spectrometer fitted with a TGS detector at Goethe University Frankfurt. Measurements were
180 performed at 1.4 cm^{-1} resolution with 32 scans. A baseline measurement was performed before
181 every sample. Before analysis, foraminifera shells were crushed using an agate pestle and mortar
182 into a fine powder. Where individual tests did not provide enough powder, two or three from the
183 same bed and of the same species were combined.

184 *Laser Ablation-ICP-MS*

185 We analysed the element/Ca ratio of four common proxies in foraminiferal calcite (B, Mg, Sr,
186 Ba), two suggested proxies yet to be widely utilised (Zn, U; Marchitto et al. 2000; Russell et al.
187 2004), and five element/Ca ratios that have been used as diagenetic indicators (Al, Mn, Y, and
188 two Rare Earth Elements (REE) - La and Ce, e.g. Pena et al. 2005; Creech et al. 2010) in both
189 Recent *O. ammonoides* and five fossil samples spanning the range of preservation states as
190 described above (Table 1). Foraminifera were analysed using the RESOlution M-50 193 nm ArF
191 laser ablation system connected to an Agilent 7500ce quadrupole mass spectrometer at Royal
192 Holloway University of London (Müller et al. 2009). Prior to analysis, samples were cleaned
193 through multiple ultrasonication steps in 18.2 MΩ deionised water, followed by a final step in
194 methanol. In addition, recent samples were first placed in 10% NaOCl until any remnant organic
195 material was oxidised. The analytical procedure and data quality for the analysis of large benthic
196 foraminifera are described at length in Evans et al. (2013; 2015). Briefly, measurements of the
197 marginal cord were performed with a 44 μm laser spot size and a fluence of 3 J/cm^2. Most
198 specimens were analysed non-destructively via slow depth-profiling of the marginal cord of

199 whole specimens mounted upright in the ablation cell, with a laser repetition rate of 2 Hz. In a
200 smaller number of cases the entire marginal cord was analysed by tracking the laser around
201 sectioned specimens at a scan speed of 1 mm/min and a repetition rate of 10 Hz. In both cases,
202 the data presented here are derived from the average of multiple analyses on at least 5-10
203 specimens. LA-ICPMS data quality is discussed in detail in (Evans and Müller 2018), briefly, the
204 accuracy and precision of Mg/Ca measurements in carbonates is <3%, and <5% for all other
205 trace elements discussed here with the exception of ^{138}Ba (precision ~10%) and ^{238}U, for which
206 precision is strongly dependent on concentration in samples such as these with very low U/Ca
207 ratios.
208
209 **RESULTS**
210 Mineralogy
211 *Modern samples*
212 Both samples of *C. carpenteri* had 2θ values of 29.8 for the calcite peak, with the KCl having an
213 exact match with its listed peak (2θ=28.3; d=3.15Å). Using the curve of Goldsmith et al. (1961)
214 a 2θ value of 29.8 corresponds to 12.8 mole% $MgCO_3$, clearly indicating a HMC composition in
215 the modern specimens. The high-Mg calcite nature of the Recent nummulitids is confirmed by
216 the LA-ICPMS Mg/Ca data. *O. ammonoides* from the GBR are characterised by a mean Mg/Ca
217 ratio of 141.5±2.2 mmol/mol (2SE population variance), equivalent to a $MgCO_3$ proportion of
218 12.4 mole%, in excellent agreement with the XRD result. More broadly, the analysis of both
219 *Operculina* and *Heterostegina* from seven globally-distributed sites conforms to this (Evans et
220 al. 2013), with reported Mg/Ca ratios between 137-155 mmol/mol (12.0-13.4 mole%). Together,

221 these results unambiguously demonstrate that the extant nummulitid foraminifera are composed
222 of HMC.
223 The FTIR spectra of the GBR *O. ammonoides* sample is characteristic of calcite, with carbonate
224 vibrations at 1084 cm^{-1} (υ_1; CO_3 symmetric stretch), 872 cm^{-1} (υ_2; out-of-plane bend), 1404 cm^{-1}
225 (υ_3; antisymmetric stretch), and 719 cm^{-1} (υ_4; in-plane bend). Note that the precise location of
226 these peaks is dependent on the composition of the calcite (Long et al. 2012). The utility of FTIR
227 to identify the Mg concentration is discussed in detail below.
228
229 *Fossil samples*
230 The well-preserved Tanzanian *Nummulites* samples from clay sediments and the echinoid
231 fragment from the same location are all characterised by 2θ values of 29.6, which corresponds to
232 6 mole% $MgCO_3$. The Bracklesham specimen also gave a 2θ value of 29.6 and 6 mole% $MgCO_3$
233 and the *N. prestwichianus* from Alum Bay 29.6 corresponding to 6 mole% $MgCO_3$. These results
234 are confirmed by the LA-ICPMS data, which yielded Mg/Ca ratios of Eocene *Nummulites*
235 between 60.9-89.8 mmol/mol for the three well-preserved samples investigated from the UK and
236 Tanzania (summarised in Fig. 2). This is equivalent to $MgCO_3$ proportions of 5.7-8.2 mole%,
237 which is slightly higher on average than the XRD results, explicable by the fact that LA-ICPMS
238 is both more precise and accurate in terms of the ability of these techniques to identify small
239 differences in Mg concentration (Table 1). These values fall between the ranges for LMC and
240 HMC, which means these samples have an intermediate composition.
241 In contrast, LBF samples that were deemed to be poorly-preserved on the basis of light
242 microscopy (see Fig. 1) are characterised by much lower and more variable Mg concentrations.

243 The XRD analysis of the Seeb specimen gave 2θ values of 29.3 from the outer part of the test
244 indicating that the mole percent $MgCO_3$ is below the limit of detection by this technique,
245 therefore it is low magnesium calcite. LA-ICPMS analysis enables the precise Mg concentration
246 to be determined, demonstrating that the sample is in fact characterised by a Mg/Ca ratio of 11
247 mmol/mol, equivalent to 1.1 mole%. In contrast, a sample of the inner whorl had a 2θ value of
248 29.6 indicating 6 mole% $MgCO_3$ and an intermediate composition. Similarly, LA-ICPMS data of
249 specimens from one of the less well-preserved Tanzania beds yielded a Mg/Ca ratio of 35
250 mmol/mol (3.4 mole%), therefore also falling within the LMC field.
251 Like the modern sample, the FTIR spectra of the fossil samples are characteristic of calcite.
252 Focusing on the υ_4 peak (in-plane bend), because it has been previously shown to be a useful
253 indicator of mineralogy (Dauphin 1999), we find that the visually well-preserved fossil material
254 has a υ_4 peak centre at 712-714 cm^{-1}, i.e. shifted to lower values by ~6 wavenumbers compared
255 to the Recent *O. ammonoides* sample. Furthermore, the visually poorly-preserved samples that
256 were determined to be LMC on the basis of XRD and LA-ICPMS analysis are characterised by a
257 narrower υ_4 full width at half maximum (FWHM), i.e. the peak width at half peak height (Table
258 1). The modern samples and well-preserved fossil material have FWHM values between 11.7-
259 13.2 cm^{-1}, whereas those from Oman and the LMC sample from Tanzania are ~35% narrower
260 (FWHM of 7.7 and 8.4 cm^{-1} respectively, see Fig. 4).
261
262 Trace Element Composition of Modern and Fossil Nummulitid Foraminifera
263 Trace element data for both modern *O. ammonoides* (from Evans et al. 2013) and fossil
264 *Nummulites* are summarised in Table 1. Here, we use the sample set to assess the role of these

265 trace elements in identifying diagenesis, and the effect of diagenesis on proxy trace element
266 systems (B, Mg, etc.). For discussion of the proxies themselves, see e.g. Katz et al. (2010), Lea
267 (2013), Evans et al. (2015), and van Dijk et al. (2017). The relatively high-concentration proxy
268 trace elements (B, Sr) are present at lower concentrations in all of the fossil samples than in
269 modern material, with the lowest concentrations in the LMC fossil material (that from Oman and
270 the limestones of Tanzania), indicating diagenetic loss. The low-concentration proxy trace
271 elements (Ba, U, Zn) are characterised by a much greater degree of variability, with values in
272 fossil material both higher and lower than modern *O. ammonoides* (Table 2). In general, the
273 fossil samples with an intermediate-Mg calcite composition have a composition similar to the
274 modern samples, whereas the composition of the LMC fossil samples is much more variable and
275 sometimes falls well outside the range of the modern material. Similarly, the trace elements often
276 used as indicators of diagenesis (e.g. Sr, Mn, Fe and REE) are present at very variable
277 concentrations, although most fossil samples are characterised by concentrations that exceed that
278 of the pristine modern material. The exception is the LMC sample from Oman, which has the
279 lowest Al/Ca ratio of any sample analysed, indicating a very low degree of clay mineral
280 contamination, and Mn, Y, La, and Ce/Ca ratios within the range of the modern samples.
281
282 **DISCUSSION**
283 Mineralogy
284 The modern specimens of *Cycloclypeus carpenteri* and *Operculina ammonoides* from all
285 methods show clear HMC values, whilst the mole% $MgCO_3$ for well-preserved fossil material
286 consistently falls within the intermediate range. At face value, this would imply that even

287 exceptionally well-preserved fossil specimens are on a diagenetic trend from HMC to LMC.
288 However, there is another factor that can control the primary Mg/Ca ratio of foraminiferal calcite
289 which must be considered. There is now abundant evidence from multiple independent archives
290 that the ratio of Mg to Ca in seawater has undergone large shifts over geological time (Stanley
291 and Hardie 1998; Horita et al. 2002; Coggon et al. 2010; Evans et al. 2018). In addition, it is
292 well-known that the composition of both inorganic and biogenic carbonate minerals are sensitive
293 to such changes, from experiments where minerals or organisms have been experimentally
294 grown in the laboratory in seawater with a non-natural composition (Mucci and Morse 1983;
295 Segev and Erez 2006; Evans et al. 2015). Specifically, reducing the Mg/Ca ratio of seawater also
296 results in a lower calcite Mg/Ca in foraminifera (Evans et al. 2015). Because the seawater Mg/Ca
297 ratio has increased by a factor of 2-3 over the Cenozoic (e.g. Coggon et al. 2010), one of the
298 main reasons that the Paleogene fossils have an intermediate mole% Mg composition whereas
299 their extant relatives are HMC is because of the changes in seawater chemistry over the
300 Cenozoic. For example, when live-collected *O. ammonoides* are cultured in seawater with a
301 Mg/Ca ratio modified to reflect that of the Palegeone reconstructions, the newly grown chambers
302 have an intermediate mole% Mg composition (Evans et al. 2015).
303 The Tanzania echinoid test fragment has a composition of 6 mole% $MgCO_3$ – the same value as
304 the well-preserved *Nummulites* from this sample. This suggests that both the *Nummulites* and
305 echinoid tests were originally of an intermediate composition. Echinoderm magnesium content in
306 modern specimens has been shown to be variable, both across species, within individual
307 skeletons and across latitudes (e.g. Chave 1954; Raupe 1966; Andersson et al. 2008; Smith et al.
308 2016) and that it also may be directly affected by changing ocean chemistry and saturation state

309 in modern oceans (Andersson et al. 2008; Hermans et al. 2010) and through geological time
310 (Smith et al. 2016). Smith et al. (2016) analysed 643 modern specimens across multiple taxa,
311 skeletal parts, and life stages, to determine an average composition of 8.9 +/- 3.7mole% $MgCO_3$
312 which means that the Eocene Tanzanian test is within error of the modern mean. Given the
313 exceptional preservation of the Tanzanian site (Bown et al. 2008), it is extremely likely that this
314 is therefore indicative of an original intermediate value.
315 The specimens from the limestone beds of Tanzania and Oman are both LMC (Table 1,
316 Fig. 2). The preservation within the limestones is poor, with specimens having been infilled, and
317 no preservation of aragonitic material (Fig. 1). This type of preservation would therefore be very
318 unlikely to preserve intermediate or HMC mineralogy. In addition, the staining of the same
319 limestone with alzarin red and potassium ferricyanide clearly shows that the *Nummulites* are
320 preserved as ferroan calcite. As iron tends to replace the magnesium in HMC during the
321 transformation to LMC (Richter and Füchtbauer 1978), these tests therefore originally had a
322 higher magnesium composition and were not LMC prior to diagenesis.
323 The combined evidence from modern and ancient specimens, coupled with the
324 comparison of echinoid test and between differing taphonomic regimes demonstrates an
325 intermediate original mineralogy in well-preserved Paleogene nummulitids and HMC in present
326 nummulitid foraminifera. That is, although the Paleogene nummulitids were characterised by
327 lower primary shell Mg/Ca ratios, the difference is driven by changes in the seawater Mg/Ca
328 ratio over the Cenozoic. In contrast, low-Mg fossil nummulitid foraminifera have undergone
329 diagenetic loss of Mg.
330

Identification of diagenesis using FTIR spectroscopy

Given that we demonstrate that both modern and well-preserved fossil nummulitids are composed of intermediate to HMC, it follows that identification of the composition of fossil material might be useful to assess whether diagenesis has taken place in shallow carbonate sections, as the presence nummulitid foraminifera would mean that some recrystallisation has taken place. In many cases poorly preserved material can be readily identified in hand specimen or via light microscopy (Fig. 1), however this is not always the case. Especially when recrystallisation takes place on the length scale of the shell microstructure, material can appear visually well-preserved yet still have undergone recrytsallisation to low-Mg calcite. For this reason, it is desirable to identify techniques that can be used to quantitatively assess visually well-preserved material.

LA-ICPMS is a highly precise technique but is relatively time consuming and not readily available to all researchers. XRD is more widely available, but is imprecise in terms of identifying $MgCO_3$ below ~6 mole%, which is close to the threshold between recrystallised samples and well-preserved Paleogene material that has a naturally lower Mg/Ca ratio due to the differences in seawater chemistry at that time. As an alternative, we explored whether FTIR spectroscopy could be employed as an extremely fast (~2 minute) method of assessing or screening fossil material.

It is well-known that the precise location of the peaks resulting from the spectroscopic analysis of materials may depend on the composition of the material analysed. For example, whilst the FTIR spectra of pure calcite and dolomite are similar, the position of the CO_3 vibrations differ (Huang and Kerr 1960). Dauphin (1999) explored the relationship between mole% $MgCO_3$ and

353 the position of the υ_4 (in-plane carbonate bend) in detail. Like Dauphin (1999), we find that the
354 υ_4 peak position is positively correlated with the Mg concentration of the sample (Fig. 3),
355 however the relatively large residuals to the best fit linear regression mean that the precision of
356 this relationship is not likely to be useful for the identification of the degree of recrystallisation
357 or Mg concentration by itself. For example, the Alum Bay sample has a υ_4 peak position just
358 ~0.5 wavenumbers higher than the poorly preserved sample from Oman, which is close to the
359 resolution of the technique. However, the FTIR peak fitting procedure (Fig. 4A,B) demonstrates
360 that well-preserved and recrystallised samples can be distinguished from one-another by using
361 both the peak centre as well as the peak width. As well as a υ_4 peak centered at lower
362 wavenumbers, the recrystallised samples have narrower υ_4 peaks, discussed in terms of the full
363 width at half maximum (FWHM) from hereon, i.e. the peak width at the position of half the peak
364 height (Table 2). In general, the mechanistic reason for this is that narrower peaks result from a
365 more homogeneous material or more ordered material, for example as Ca-O and Mg-O have
366 differing bond distances, calcite with a greater $MgCO_3$ proportion also has a greater bulk
367 heterogeneity in the CO_3 vibration modes.
368 Regressing the υ_4 FWHM against peak position (Fig. 4D) demonstrates how the two pieces of
369 information can be used together to identify intermediate or HMC that has undergone diagenetic
370 recrystallisation. Well-preserved samples are distinct from visually poorly-preserved material in
371 that they are characterised by a υ_4 peak width ~4 wavenumbers narrower than the well-preserved
372 material in all cases, as expected for a more homogeneous material. In contrast, the well-
373 preserved fossil and modern material have similar υ_4 FWHM, but a wider range in the υ_4 peak
374 position, which may therefore help to distinguish mole% Mg at higher percentages. Therefore,

375 recrystallised samples may be readily identified using this technique as they are distinct in terms
376 of their υ_4 peak characteristics, specifically, being characterised by a narrow peak at ~712 cm^{-1}
377 rather than a wider peak at 712-720 cm^{-1}. We stress that measured FWHM is somewhat
378 dependent on the spectral resolution of the instrument being used, such that the absolute values
379 should be determined for well-preserved and recrystallised material on a given system before this
380 technique is employed. Nonetheless, the method offers a fast, simple method of detecting
381 diagenesis in intermediate/high magnesium calcite, without the need for complex sample
382 preparation in a clean environment beyond standard laboratory good practice.
383
384 On the use of trace element data to determine sample preservation
385 Trace element proxies in foraminiferal calcite have been widely applied over a range of
386 timescales to reconstruct the environmental conditions during the life of the organism. The most-
387 widely utilised example being the application of the empirical relationship between the Mg/Ca
388 ratio and temperature, which forms the basis of a large portion of our knowledge of ocean
389 temperatures in the past (e.g. Nürnberg et al. 1996; Rosenthal et al. 1997). The fidelity of these
390 proxies as analysed in fossil material depends on such archives maintaining their original
391 composition over geological time. However, processes such as dissolution (Fehrenbacher and
392 Martin 2014), the precipitation of secondary inorganic overgrowths (Pena 2005), recrystallisation
393 (Evans et al. 2015), and contamination by (e.g.) clay minerals mean that this is not always the
394 case. As such, an essential part of utilising the geochemistry of fossil foraminifera as
395 palaeoclimate archives is understanding the extent to which these faithfully record their primary
396 composition (Pearson et al. 2001).

With the advent of inductively coupled plasma techniques facilitating the simultaneous collection of a large number of major and trace elements, carbonate preservation is frequently assessed by the establishment of geochemical 'fingerprints' of the diagenetic endmembers described above. For example, secondary overgrowths are typically enriched in manganese relative to foraminiferal carbonate (Pena et al. 2005), such that Mn/Ca ratios can be used to assess this aspect of diagenesis whilst simultaneously collecting the proxy trace element data of interest. Likewise, Al, or Fe/Ca ratios can be indicative of clay mineral (aluminosilicate) contamination, Sr is typically lost during dissolution (Stoll et al. 1999), and recrystallised foraminifera typically have increased rare earth element (REE) concentrations (Evans et al. 2015). Here, we revisit the utility of these preservational indicators because 1) we deliberately analysed foraminifera from a wide range of preservational states which means that the efficacy of these indicators can be tested, and 2) the HMC original mineralogy of the *Nummulites*, which recrystallises to LMC during diagenesis, means that unlike the low-Mg species, we can independently assess recrystallisation and examine diagenetic indicators within this context.

To assess geochemical preservation, we compare our data to modern *O. ammonoides* for two reasons. Firstly, these samples cannot be diagenetically altered and therefore provide a pristine endmember to which the fossil material can be compared. Secondly, it is probable that all biologically-precipitated calcites are geochemically fractionated compared to inorganic calcite, either because the organism modifies the chemistry at the site of calcification, or because the higher precipitation rate of biological precipitation results in more extreme kinetic fractionations (Bentov and Erez 2006; Dellinger et al., 2018). Within the benthic foraminifera in general, the high-Mg nummulitids nonetheless have a composition relatively close to inorganic calcite

419 (Evans et al. 2015), implying a relatively low degree of biological fractionation. In addition,
420 fossil *Operculina* and *Nummulites* have a major/trace element composition that is identical
421 within uncertainty where they occur together in the same bed (Evans et al. 2013) and likewise,
422 no offsets have been observed between different species of the modern nummulitid foraminifera
423 (*O. ammonoides*, *O. complanata*, *Heterostegina depressa*), see Evans et al. (2015). Given the
424 above, we assess geochemical differences between the fossil samples by comparing the fossil
425 analyses to pristine modern material. Specifically, we calculate ratios for each element as R_X =
426 $(X/Ca_{fossil})/(X/Ca_{\textit{Operculina}})$, where X is the element of interest, relative to Ca as is convention
427 when reporting carbonate trace element data, and $X/Ca_{\textit{Operculina}}$ is the average value for modern
428 *O. ammonoides*. *Operculina ammonoides* is used here as the modern nummulitid representative
429 because trace element data are available from multiple globally-spaced samples from Evans et al.
430 (2013), which means that our analysis is not biased by considering modern foraminifera from
431 only one location. Within this framework, an R_X value <1 would imply either diagenetic loss of
432 that element from the foraminifer shell, or that the element was originally incorporated into the
433 calcite to a lesser extent, which could be related to a multitude of environmental or biological
434 factors (see e.g. Rosenthal et al. 1997; Russell et al. 2004; Evans et al. 2015; van Dijk et al.
435 2017).
436 In Figure 5, the elements are ordered from left to right first by their use as proxies (B, Mg, Zn,
437 Sr, Ba, U on the left, diagenetic indicators on the right), and then within those groups, by the
438 approximate ease with which the concentration of these elements can be altered away from
439 primary values. For example, boron in foraminiferal calcite is thought to be relatively resistant to
440 diagenesis (Edgar et al. 2015), whereas U and Zn are low concentration trace elements, such that

441 even a small degree of diagenetic alteration can shift measured values in calcite away from that
442 of pristine foraminifera. Al is positioned first in the sequence of diagenesis indicators because in
443 most cases the clay removal cleaning step should result in very little clay contamination,
444 followed by Mn, Y and the REE in order of their approximate concentration in pristine
445 foraminiferal calcite (i.e. foraminiferal Ce concentrations are more likely to be altered compared
446 to Y, because Ce is present at a lower concentration). We term this figure the 'carbonate
447 preservagram', and suggest that it could be routinely used to enable a more comprehensive
448 overview of the degree and style of diagenetic alteration for the reasons outlined below.
449 The aim of this exercise (Fig. 5) is to identify the manifestation of patterns of trace element
450 preservation under different preservational states and to identify possible instances for which
451 diagenesis proxies may not be reliable indicators of recrystallisation. However, care should be
452 taken in interpreting the details of this diagram because environmental changes will also have
453 imparted a control on the primary composition of these carbonates. For example, changes in
454 seawater chemistry and temperature result in lower Eocene nummulitid Mg/Ca ratios compared
455 to modern, such that the lower Mg/Ca ratios of the well-preserved fossil data do not necessarily
456 imply diagenetic alteration. For example, the Eocene seawater Mg/Ca ratio was ~2.5 times lower
457 than at present, whereas the seawater B/Ca ratio was 20% lower (Lemarchand et al. 2002; Evans
458 et al. 2018). Indeed, all three of the well-preserved samples (Tanzania, Barton, Bracklesham) are
459 characterised by lower B/Ca, Mg/Ca and Sr/Ca ratios than modern *O. ammonoides* which can be
460 related to these independent reconstructions of changes in seawater chemistry (i.e. a lower pH,
461 lower boron, and higher calcium concentration in the Eocene compared to today, see Stanley and
462 Hardie 1998; Lemarchand et al. 2002; Anagnostou et al. 2016), and we examine the data in this

463 context. Aside from the proxy trace elements already discussed, the U/Ca ratios of the well-
464 preserved fossil samples fall within the range of the modern *O. ammonoides* (Fig. 5), whereas
465 Zn/Ca is more highly variable, implying that these samples may retain their primary U
466 concentrations, but this is not always the case for Zn even in exceptional material. The
467 diagenesis indicators show a general upward trend from Al and Mn to the REE, which suggests
468 that even in these samples minor diagenetic processes, likely minor secondary mineral
469 precipitation, have resulted in elevated concentrations. Crucially though, there is no evidence
470 that these minor phases have impacted the proxy trace elements of interest.
471 The two poorly preserved samples, from the late Eocene of Tanzania and Oman, both show
472 diagenetic loss of the higher concentration proxy trace elements (B, Mg, Sr), by analogy to both
473 the modern and well-preserved Paleogene material. The late Eocene sample from Tanzania has
474 Al and Mn/Ca ratios comparable to the well-preserved material, but shows clear diagenetic gain
475 of Y and the REE, and U, with Ce/Ca almost 100 times higher than in modern *O. ammonoides*.
476 Together with the diagenetic loss of Mg, Figure 5 shows how a suite of elements can be used to
477 identify this sample as poorly preserved despite the fact that the 'traditional' indicators of
478 diagenesis (Al, Mn), would not cause this sample to be screened out. The sample from Oman
479 clearly underwent a distinct diagenetic history, with virtually all of the diagenesis proxies present
480 at similar, or even lower, concentrations than the pristine modern material, with only U
481 significantly elevated in this material compared to the well-preserved fossil samples. In fact, the
482 poor preservation of this material is best evidenced by the proxy trace elements, all present at
483 levels 5-10 times lower than the modern samples, and at least 2 times lower than the well-
484 preserved fossil material. In practical terms, this assessment is also clearly backed up by the

visually recrystallised and partially infilled nature of this material, as well as the FTIR analysis presented in Sec. 4.2.

Overall, this exercise demonstrates that no single trace element system, and moreover, no combination of diagenesis proxies can unambiguously identify significant diagenetic alteration in all cases. Indeed, the worst-preserved material studied here (from Oman), is the only fossil sample to have almost all measured trace element diagenesis indicators at or below the range of pristine modern material (Al, Mn, Y, the REE). Clearly, trace element data alone are not a complete substitute for other techniques such as SEM imaging (e.g. Pearson et al. 2001) or spectral techniques. However, we suggest that carbonate preservagrams (Fig. 5) could be used to identify patterns of diagenesis, or to aid in the identification of samples which are not well-preserved by analogy to the nearest living relative or approximately coeval fossil material known to be well-preserved on the basis of alternative techniques. Many laboratories routinely analyse the REE and U as well as Al and Mn, such that presenting the data in this way would strengthen the interpretation regarding preservation, or enable poorly preserved samples to be screened out on the basis of a suite of trace elements rather than single diagenetic indicators such as Al or Mn which are informative only in certain settings (Fig. 5).

CONCLUSIONS

All chemical analyses carried out to determine nummulitid mineralogy clearly show modern relatives of *Nummulites* have a HMC composition and exceptionally preserved Eocene fossil material to be of intermediate Mg content. Given data from culturing experiments which show that mole% Mg in these, and indeed all foraminifera, is strongly influenced by the seawater

507 Mg/Ca ratio. Coupled with our knowledge of Paleogene ocean chemistry, this strongly suggests
508 *Nummulites* and nummulitids were of an intermediate $MgCO_3$ composition during the Eocene as
509 a result of the lower seawater Mg/Ca ratio at the time, compared to the modern HMC relatives.
510 This is additionally supported by the Mg concentration of the echinoderm test fragment which is
511 at the lower end of modern values. This confirmation of the composition of nummulitid tests
512 allows for a more accurate assessment of material used for isotopic and geochemical studies, a
513 field in which they are increasingly being used.
514 We have additionally shown that FTIR spectroscopy may offer a relatively quick, easy
515 and inexpensive method of assessing preservation in specimens, although it is system dependent
516 and thus a calibration for the individual set-up is required before analysis is carried out. Lastly,
517 we highlight that LA-ICPMS trace element data of variably preserved samples is complex, with
518 poorly preserved material from Oman having similar levels of some trace elements as modern
519 specimens, and therefore advocate for suites of elements and comparison to closest modern
520 relatives to be used rather than relying on singly diagenetic indicators. Carbonate preservagrams,
521 in this way, could therefore aid in diagenetic assessment.
522
523 ACKNOWLEDGEMENTS
524 We thank Anthony Oldroyd (Cardiff University) for running XRD analysis. COSTECH and
525 Tanzania Petroleum Drilling Coorporation are acknowledged for their assistance with the
526 Tanzania Drilling Project. We are grateful to Paul Webb for help with ATR-FTIR spectroscopy,
527 and Wolfgang Müller for making the LA-ICPMS analyses possible. SJB-P thanks Johann

528 Hohenegger (University of Vienna) for the modern nummulitid samples. We thank two
529 anonymous reviewers for their helpful comments that improved the manuscript.
530
531 REFERENCES
532 ANAGNOSTOU, E., JOHN, E.H., EDGAR, K.M., FOSTER, G.L., RIDGWELL, A., INGLIS, G.N.,
533 PANCOST, R.D., LUNT, D.J., and PEARSON, P.N., 2016, Changing atmospheric CO2
534 concentration was the primary driver of early Cenozoic climate: Nature, doi:
535 10.1038/nature17423.
536 ANDERSSON, A. J., MACKENZIE, F. T. and BATES, N. R., 2008, Life on the margin: implications
537 of ocean acidification on Mg calcite, high latitude and cold-water marine calcifiers: Mar
538 Ecol Prog Ser., v. 373, pp. 265−273.
539 BATHURST, R. G., 1976, Carbonate sediments and their diagenesis, Development in
540 sedimentology: Elsevier, Amsterdam
541 BLACKMON, P.D. and TODD, R., 1959, Mineralogy of some foraminifera as related to their
542 classification and ecology: Journal of Paleontology, p.1-15.
543 BEAVINGTON-PENNEY, S.J., and RACEY, A., 2004, Ecology of extant nummulitids and other
544 larger benthic foraminifera: Applications in palaeoenvironmental analysis: Earth-Science
545 Reviews, v. 67, p. 219–265, doi: 10.1016/j.earscirev.2004.02.005.
546 BEAVINGTON-PENNEY, S.J., WRIGHT, V. P, and RACEY, A., 2006, The middle Eocene Seeb
547 Formation of Oman: an investigation of acyclicity, stratigraphic completeness and
548 accumulation rates in shallow marine carbonate settings: Journal of Sedimentary Research,
549 v. 76, p. 1137-1161.
550 BEAVINGTON-PENNEY, S.J., NADIN, P., WRIGHT, V. P., CLARKE, E., MCQUILKEN, J., and BAILEY,

551 H. W., 2008, Reservoir quality variation on an Eocene carbonate ramp, El Garia Formation,
552 Offshore Tunisia: structural control of burial corrosion and dolomitisation: Sedimentary
553 Geology, v. 209, p. 42–57
554 BENEDETTI, A., LESS, G., PARENTE, M., PIGNATTI, J., CAHUZAC, B., TORRES-SILVA, A.I. AND
555 BUHL, D., 2018, *Heterostegina matteuccii* sp. nov.(Foraminiferida: Nummulitidae) from the
556 lower Oligocene of Sicily and Aquitaine: a possible transatlantic immigrant: Journal of
557 Systematic Palaeontology, v. 16(2), p. 87–110.
558 BENTOV, S., AND EREZ, J., 2006, Impact of biomineralization processes on the Mg content of
559 foraminiferal shells: A biological perspective: Geochemistry, Geophysics, Geosystems, v.
560 7(1), Q01P08, doi:10.1029/2005GC001015.
561 BLONDEAU, A., 1972, Les nummulites. De l'enseignement a la récherche des sciénces
562 de la terre: Paris, Vuibert, pp. 1-254.
563 BOWN, P.R., JONES, T.D., LEES, J.A., RANDELL, R.D., MIZZI, J.A., PEARSON, P.N., COXALL,
564 H.K., YOUNG, J.R., NICHOLAS, C.J., KAREGA, A., SINGANO, J., and WADE, B.S., 2008, A
565 Paleogene calcareous microfossil Konservat-Lagerstätte from the Kilwa Group of coastal
566 Tanzania: Bulletin of the Geological Society of America, v. 120, p. 3–12, doi:
567 10.1130/B26261.1.
568 BRENCHLEY, P.J. and HARPER, D.A.T., 1998, Palaeoecology: Ecosystems, Environments and
569 Evolution: Chapman and Hall, London.
570 CHAVE, K.E., 1954, Aspects of the biogeochemistry of magnesium 1. Calcareous marine
571 organisms: The Journal of Geology, v. 62, p.266-283.
572 COGGON, R.M., TEAGLE, D. a H., SMITH-DUQUE, C.E., ALT, J.C., and COOPER, M.J., 2010,
573 Reconstructing past seawater Mg/Ca and Sr/Ca from mid-ocean ridge flank calcium

carbonate veins.: Science (New York, N.Y.), v. 327, p. 1114–7, doi: 10.1126/science.1182252.

COTTON, L. J., RIVERO-CUESTA, L., FRANCESCHETTI, G., IAKOVLEVA, A., ALEGRET, L., DINARÈS-TURELL, J., HOOKER, J., KING, C., FLUEGEMAN, R., YAGER, S. and MONECHI, S., 2020, Reassessing the Bartonian unit stratotype at Alum Bay (Isle of Wight, UK): an integrated approach: Newsletters on stratigraphy, in press.

COTTON, L.J., and PEARSON, P.N., 2011, Extinction of larger benthic foraminifera at the Eocene/Oligocene boundary: Palaeogeography, Palaeoclimatology, Palaeoecology, v. 311, p. 281–296, doi: 10.1016/j.palaeo.2011.09.008.

CREECH, J.B., BAKER, J. a., HOLLIS, C.J., MORGANS, H.E.G., and SMITH, E.G.C., 2010, Eocene sea temperatures for the mid-latitude southwest Pacific from Mg/Ca ratios in planktonic and benthic foraminifera: Earth and Planetary Science Letters, v. 299, p. 483–495, doi: 10.1016/j.epsl.2010.09.039.

CURRY, D., KING, A. D., KING, C., and STINTON, F. C., 1977, The Bracklesham Beds (Eocene) of Bracklesham Bay and Selsey, Sussex: Geological Association London, Proceedings, v. 88, p. 243–254.

DEBENAY, J.P., GUILLOU, J.J., GESLIN, E. and LESOURD, M., 2000, Crystallization of calcite in foraminiferal tests: Micropaleontology, v. 46, p.87–94.

DAUPHIN, Y., 1999, Infrared Spectra and Elemental C omposition in Recent Biogenic C alcites : Relationships between the n 4 Band Wavelength and Sr and Mg C oncentrations: v. 53, p. 184–190.

DELLINGER, M., WEST, A. J., PARIS, G., ADKINS, J. F., VON STRANDMANN, P. A. P., ULLMANN, C. V., AND CORSETTI, F. A., 2018, The Li isotope composition of marine biogenic carbonates:

597 Patterns and Mechanisms: Geochimica et Cosmochimica Acta, v. 236, p. 315–335.
598 VAN DIJK, I., DE NOOIJER, L.J., and REICHART, G.-J., 2017, Trends in element incorporation in
599 hyaline and porcelaneous foraminifera as a function of
600 <i>p</i>CO₂
601 Biogeosciences, v. 14, p. 497–510, doi: 10.5194/bg-14-497-2017.
602 EDGAR, K.M., ANAGNOSTOU, E., PEARSON, P.N., and FOSTER, G.L., 2015, Assessing the impact
603 of diagenesis on δ11B, δ13C, δ18O, Sr/Ca and B/Ca values in fossil planktic foraminiferal
604 calcite: Geochimica et Cosmochimica Acta, v. 166, p. 189–209, doi:
605 10.1016/j.gca.2015.06.018.
606 EVANS, D., EREZ, J., ORON, S., and MÜLLER, W., 2015, Mg/Ca-temperature and seawater-test
607 chemistry relationships in the shallow-dwelling large benthic foraminifera Operculina
608 ammonoides: Geochimica et Cosmochimica Acta, v. 148, p. 325–342, doi:
609 10.1016/j.gca.2014.09.039.
610 EVANS, D., and MÜLLER, W., 2018, Automated Extraction of a Five-Year LA-ICP-MS Trace
611 Element Data Set of Ten Common Glass and Carbonate Reference Materials: Long-Term
612 Data Quality, Optimisation and Laser Cell Homogeneity: Geostandards and Geoanalytical
613 Research, doi: 10.1111/ggr.12204.
614 EVANS, D., MÜLLER, W., ORON, S., and RENEMA, W., 2013, Eocene seasonality and seawater
615 alkaline earth reconstruction using shallow-dwelling large benthic foraminifera: Earth and
616 Planetary Science Letters, v. 381, p. 104–115, doi: 10.1016/j.epsl.2013.08.035.
617 EVANS, D., SAGOO, N., RENEMA, W., COTTON, L.J., MÜLLER, W., TODD, J.A., SARASWATI, P.K.,
618 STASSEN, P., ZIEGLER, M., PEARSON, P.N., VALDES, P.J., and AFFEK, H.P., 2018, Eocene
619 greenhouse climate revealed by coupled clumped isotope-Mg/Ca thermometry: Proceedings

620 of the National Academy of Sciences, v. 115, p. 1174–1179, doi:
621 10.1073/pnas.1714744115.
622 EVANS, D., MÜLLER, W., AND EREZ, J., 2018, Assessing foraminifera biomineralisation models
623 through trace element data of cultures under variable seawater chemistry: Geochimica et
624 Cosmochimica Acta, v. 236, p. 198–217.
625 FEHRENBACHER, J.S., and MARTIN, P.A., 2014, Exploring the dissolution effect on the intrashell
626 Mg/Ca variability of the planktic foraminifer Globigerinoides ruber: p. 1–15, doi:
627 10.1002/2013PA002571.Received.
628 GOLDSMITH, J. R., GRAF, D. and HEARD, H. C., 1961, Lattice constants of the calcium
629 magnesium carbonates: American Mineralogist, v. 46, p. 453–457.
630 HALLOCK, P., PREMOLI, S.I. and BOERSMA, A., 1991., Similarities between planktonic and larger
631 foraminiferal evolutionary trends through Paleogene palaeoceanographic change:
632 Palaeogeography, Palaeoclimate, Palaeoecology, v. 83, p. 49–64.
633 HERMANS, J., BORREMANS, C.,, WILLENZ, P., ANDRÉ, L. and DUBOIS, P., 2010, Temperature,
634 salinity and growth rate dependences of Mg/Ca and Sr/Ca ratios of the sea urchin
635 *Paracentrotus lividus* (Lamarck): an experimental approach: Marine Biology, v. 157, p.
636 1293−1300.
637 HOHENEGGER, J., YORDANOVA, E. and HATTA, A., 2000, Remarks on west Pacific Nummulitidae
638 (foraminifera): The Journal of Foraminiferal Research, v. 30(1), p. 3–28.
639 HOLAIL, H., 1994, Diagenesis of the middle Eocene “Nummulite bank” of The Giza Pyramids
640 Plateau, Egypt: Petrologic and 18O/16O evidence: Qatar University Science Journal, p.
641 146–452.
642 HORITA, J., ZIMMERMANN, H., and HOLLAND, H.D., 2002, Chemical evolution of seawater

643 during the Phanerozoic : Implications from the record of marine evaporites: Geochimica et
644 Cosmochimica Acta, v. 66, p. 3733–3756.
645 HUANG, C.K., and KERR, P.F., 1960, Infrared study of the carbonate minerals: The American
646 Mineralogist, v. 4, p. 311–324.
647 JAMES, N.P., COLLINS, L.B., BONE, Y., and HALLOCK, P., 1999, Subtropical carbonates in a
648 temperate realm; modern sediments on the Southwest Australian shelf: Journal of
649 Sedimentary Research, v. 69, p. 1297–1321, doi: 10.2110/jsr.69.1297.
650 KATZ, M.E., CRAMER, B.S., FRANZESE, a., HONISCH, B., MILLER, K.G., ROSENTHAL, Y., and
651 WRIGHT, J.D., 2010, Traditional and Emerging Geochemical Proxies in Foraminifera: The
652 Journal of Foraminiferal Research, v. 40, p. 165–192, doi: 10.2113/gsjfr.40.2.165.
653 LEA, D.W., 2013, Elemental and Isotopic Proxies of Past Ocean Temperatures: Elsevier Ltd.,
654 373–397 p.
655 LEMARCHAND, D., GAILLARDET, J., LEWIN, E., AND ALLEGRE, C. J., 2002, Boron isotope
656 systematics in large rivers: implications for the marine boron budget and paleo-pH
657 reconstruction over the Cenozoic: Chemical Geology, v. 190, p. 123–140.
658 LESS, G., ÖZCAN, E., PAPAZZONI, C.A., AND STOCKAR, R., 2008, The middle to late Eocene
659 evolution of nummulitid foraminifer *Heterostegina* in the Western Tethys: Acta
660 Palaeontologica Polonica, v. 53(2), p. 317–350
661 LONG, X., NASSE, M.J., MA, Y., and QI, L., 2012, From synthetic to biogenic Mg-containing
662 calcites: A comparative study using FTIR microspectroscopy: Physical Chemistry Chemical
663 Physics, v. 14, p. 2255–2263, doi: 10.1039/c2cp22453d.
664 MACAULEY, C.I., BECKETT, D., BRAITHWAITE, K., BLIEFNICK, D. and PHILPS, B., 2001,
665 Constraints on diagenesis and reservoir quality in the fractured Hasdrubal field, offshore

Tunisia: Journal of Petroleum Geology, v. 24, p. 55–78.

MARCHITTO, T., CURRY, W., and OPPO, D., 2000, Zinc concentrations in benthic foraminifera reflect seawater chemistry: Paleoceanography.

MILLIMAN, J.D., 1974, Recent Marine Carbonates: Springer-Verlag, Berlin Heidelberg, 363 pp.

MUCCI, A., and MORSE, J.W., 1983, The incorporation of Mg2+ and Sr2+ into calcite overgrowths: influences of growth rate and solution composition: Geochimica et Cosmochimica Acta, v. 47, p. 217–233, doi: 10.1016/0016-7037(83)90135-7.

MÜLLER, W., SHELLEY, M., MILLER, P., and BROUDE, S., 2009, Initial performance metrics of a new custom-designed ArF excimer LA-ICPMS system coupled to a two-volume laser-ablation cell: J. Anal. At. Spectrom., v. 24, p. 209–214, doi: 10.1039/B805995K.

NICHOLAS, C.J., PEARSON, P.N., BOWN, P.R., JONES, T.D., HUBER, B.T., KAREGA, A., LEES, J.A., MCMILLAN, I.K., O'HALLORAN, A., SINGANO, J.M., and WADE, B.S., 2006, Stratigraphy and sedimentology of the Upper Cretaceous to Paleogene Kilwa Group, southern coastal Tanzania: Journal of African Earth Sciences, v. 45, p. 431–466, doi: 10.1016/j.jafrearsci.2006.04.003.

NÜRNBERG, D., BIJMA, J., and HEMLEBEN, C., 1996, Assessing the reliability of magnesium in foraminiferal calcite as a proxy for water mass temperatures: Geochimica et Cosmochimica Acta, v. 60, p. 803–814, doi: 10.1016/0016-7037(95)00446-7.

PAPAZZONI, C.A., 1998, Biometric analyses of *Nummulites "ptukhiani"* Z. D. Kacharava, 1969 and *Nummulites fabianii* (Prever in fabiani, 1905): Journal of Foraminiferal Research, v. 28, p. 161–176.

PAPAZZONI, C.A., ĆOSOVIĆ, V., BRIGUGLIO, A. AND DROBNE, K., 2017, Towards a calibrated larger foraminifera biostratigraphic zonation: celebrating 18 years of the application of

shallow benthic zones: Palaios, v. 32(1), p.1–4.

PEARSON, P.N., DITCHFIELD, P.W., SINGANO, J., HARCOURT-BROWN, K.G., NICHOLAS, C.J., OLSSON, R.K., SHACKLETON, N.J., and HALL, M. a, 2001, Warm tropical sea surface temperatures in the Late Cretaceous and Eocene epochs.: Nature, v. 413, p. 481–7, doi: 10.1038/35097000.

PEARSON, P.N., MCMILLAN, I.K., WADE, B.S., JONES, T.D., COXALL, H.K., BOWN, P.R., and LEAR, C.H., 2008, Extinction and environmental change across the Eocene-Oligocene boundary in Tanzania: Geology, v. 36, p. 179–182, doi: 10.1130/G24308A.1.

PENA, L.D., 2005, Identification and removal of Mn-Mg-rich contaminant phases on foraminiferal tests: Implications for Mg/Ca past temperature reconstructions: Geochemistry Geophysics Geosystems, v. 6, doi: 10.1029/2005GC000930.

PURTON, L., 1997, Gastropod carbonate δ 18 O and δ 13 C values record strong seasonal productivity and stratification shifts during the late Eocene in England: October, p. 871–874.

PURTON, L.M.A., and BRASIER, M.D., 1999, Giant protist Nummulites and its Eocene environment : Life span and habitat insights from δ 18 O and δ 13 C data from Nummulites and Venericardia , Hampshire basin , UK: p. 711–714.

RACEY, A., 1994, Biostratigraphy and palaeobiogeographic significance of Tertiary nummulitid (foraminifera) from northern Oman, *in* Simmons, M.D. (ed.), Micropalaeontology and Hydrocarbon Exploration in the Middle East: Chapman- Hall, London, p. 343-370.

RACEY, A., 1995, Lithostratigraphy and larger foraminferal (nummulitic) biostratigraphy of the Tertiary of northern Oman: Micropaleontology, v. 41, supplement p. 1-123.

RACEY, A., 2001, A review of Eocene nummulite accumulations:structure, formation and

712 reservoir potential: Journal of Petroleum Geology, v. 24, p. 79–100.
713 RAUP, D. M., 1966, The endoskeleton, *in* Boolootian RA (ed), Physiology of Echinodermata:
714 John Wiley and Sons Inc, New York, p. 379−395
715 RENEMA, W., BEAMAN, R.J., and WEBSTER, J.M., 2013, Mixing of relict and modern tests of
716 larger benthic foraminifera on the Great Barrier Reef shelf margin: Marine
717 Micropaleontology, v. 101, p. 68–75, doi: 10.1016/j.marmicro.2013.03.002.
718 RICHTER, D.K. and FÜCHTBAUER, H., 1978, Ferroan calcite replacement indicates former
719 magnesian calcite skeletons: Sedimentology, v. 25(6), p.843–860.
720 ROSENTHAL, Y., BOYLE, E. a., and SLOWEY, N., 1997, Temperature control on the incorporation
721 of magnesium, strontium, fluorine, and cadmium into benthic foraminiferal shells from
722 Little Bahama Bank: Prospects for thermocline paleoceanography: Geochimica et
723 Cosmochimica Acta, v. 61, p. 3633–3643, doi: 10.1016/S0016-7037(97)00181-6.
724 RUSSELL, A.D., HÖNISCH, B., SPERO, H.J., and LEA, D.W., 2004, Effects of seawater carbonate
725 ion concentration and temperature on shell U, Mg, and Sr in cultured planktonic
726 foraminifera: Geochimica et Cosmochimica Acta, v. 68, p. 4347–4361, doi:
727 10.1016/j.gca.2004.03.013.
728 SEGEV, E., and EREZ, J., 2006, Effect of Mg/Ca ratio in seawater on shell composition in shallow
729 benthic foraminifera: Geochemistry Geophysics Geosystems, v. 7, p. 1–8, doi:
730 10.1029/2005GC000969.
731 SEN GUPTA, B.K.,1999, Systematics of modern foraminifera, *in* Sen Gupta, B.K. (Ed.), Modern
732 Foraminfera: Kluwer Academic Publishers, Dordrecht, p. 7–36.
733 SERRA-KIEL, J., HOTTINGER, L., CAUS, E., DROBNE, K., FERRANDEZ, F., JAUHRI, A.K., LESS, G.,
734 PAVLOVEC, R., PIGNATTI, J., SAMSO, J.M., SCHAUB, H., SIREL, E., STROUGO, A.,

735 TAMBAREAU, Y., et al., 1998, Larger foraminiferal biostratigraphy of the Tethyan Paleocene
736 and Eocene: Bull. Soc. géol. France, v. 169, p. 281–299.
737 SMITH, A.M., CLARK, D.E., LAMARE, M.D., WINTER, D.J., and BYRNE, M., 2016, Risk and
738 resilience: Variations in magnesium in echinoid skeletal calcite: Marine Ecology Progress
739 Series, v. 561, p. 1–16, doi: 10.3354/meps11908.
740 STANLEY, S.M., and HARDIE, L.A., 1998, Secular oscillations in the carbonate mineralogy of
741 reef-building and sediment-producing organisms driven by tectonically forced shifts in
742 seawater chemistry: Palaeogeography, Palaeoclimatology, Palaeoecology, v. 144, p. 3–19,
743 doi: 10.1016/S0031-0182(98)00109-6.
744 STOLL, H.M., SCHRAG, D.P., and CLEMENS, S.C., 1999, Are seawater Sr/Ca variations preserved
745 in Quaternary foraminifera? Geochimica et Cosmochimica Acta, v. 63, p. 3535–3547, doi:
746 10.1016/S0016-7037(99)00129-5.
747 WEFER, G., and BERGER, W., 1980, Stable isotopes in benthic foraminifera: seasonal variation in
748 large tropical species: Science, v. 209, p. 803.
749 WHITTLE, G.L., and ALSHARHAN, A.S., 1994, Dolomitization and chertification of the Early
750 Eocene Rus Formation in Abu Dhabi, United Arab Emirates: Sedimentary Geology, v. 92,
751 p. 273–285, doi: 10.1016/0037-0738(94)90110-4.
752
753 FIGURE CAPTIONS
754
755 FIG. 1. — Examples of fossil *Nummulites* included in the study. **A)** Well-preserved specimen of
756 reticulate *Nummulites* from Tanzania (~1.25 mm diameter). **B)** specimen of *Nummulites* from the
757 Seeb formation, Oman (~15 mm diameter). **C)** *Nummulites prestwichianus* from Alum Bay, UK

(~1.5 mm diameter). **D)** *Nummulites* c.f. *fichteli* from Tanzania in equatorial section showing excellent preservation (scale bar 0.5 mm). **E)** *Nummulites* c.f. *fabianii* from Tanzania in equatorial section showing poor preservation (scale bar 0.5 mm). **F)** Scanning electron microscope image of modern *Cycloclypeus* (scale bar 0.2 mm). **G)** Scanning electron microscope image of *Nummulites laevigatus* from the Bracklesham group, U.K (scale bar 0.5 mm). **H)** Group of average to poorly preserved reticulate *Nummulites* from Tanzania (~ 1- 4 mm diameter). **I)** Petrological thin section of Seeb formation.

FIG. 2. — Overview of the composition of fossil and Recent nummulitid foraminifera (see Table 1). The approximate boundaries between low-Mg, intermediate, and high-Mg calcite are given by horizontal dashed lines. GBR – Great Barrier Reef.

FIG. 3. — Utility of the υ_4 FTIR peak centre (CO_3 in-plane bend) to constrain the Mg concentration of calcite. Data from Dauphin (1999) - coralline algae, brachiopods, sea urchins and speleothem calcite - are shown in comparison to nummulitid samples from this study.

FIG. 4. — Overview of FTIR results and peak fitting exercise. **A)** Representative FTIR spectra of exceptionally-preserved nummulitid calcite (earliest Oligocene of Tanzania). **B)** Expanded view of the υ_4 peak (CO_3 in-plane bend, see box in panel A), showing the peak-fitting strategy. A two-peak fit was used because the υ_4 peak is asymmetric, the peak located on the higher wavenumber side was used for analysis. **C)** υ_4 region of all samples (see Table 1). Those with dashed lines are samples that were deemed poorly preserved on the basis of light microscopy. **D)** Comparison of the υ_4 peak centre and full width at half maximum (FWHM) for all samples, based on the fitting

781 procedure shown in panel B. Symbol colour is shown as a function of the LA-ICPMS derived
782 shell Mg/Ca ratio.
783
784 FIG. 5. — Trace and major element data of variously-preserved Eocene *Nummulites*.
785 Concentrations are plotted as a ratio to the average value of the nearest living relatives, see text
786 for details. The grey shaded region shows the natural range of modern samples from several
787 globally-distributed sites (see Evans et al. 2015). In this context, a value of 10 would imply an
788 element/Ca ratio 10 times higher in the fossil material than in the modern samples, whereas a
789 value of 0.1 would imply a ratio 10 times lower. Offsets from a value of 1 could either be due to
790 diagenetic alteration or changes in the original composition of the shell, for example as a result
791 of a different seawater chemistry when the organism was alive compared to today. The aim of
792 the diagram is to assess diagenesis across a suite of both proxy elements (B, Mg, Sr, Ba, U, Zn)
793 and those commonly used as an indication of preservation (Al, Mn, Y, the REE), in order to gain
794 a broader understanding of how different diagenetic settings impact the overall geochemistry of
795 foraminifera. Proxy trace/major elements are very approximately placed in order of increasing
796 susceptibility to diagenesis, followed by Al (an indication of clay mineral contamination), and
797 then diagenetic indicators in approximate order of decreasing concentration in foraminiferal
798 calcite. Note that data are connected by lines to aid readability, but this does not necessarily
799 imply that adjacent trace element systems are closely linked in terms of their response to
800 diagenetic processes.
801

802 TABLE 1. — Modern and fossil shell chemistry and selected FTIR data with utility for the
803 identification of calcite composition (the υ_4 in-plane bend peak position and full width at half
804 maximum (FWHM))
805
806 TABLE 2 — Modern and fossil shell trace element. All values are given as element/Ca ratios in
807 μmol/mol, with the exception of Sr/Ca which is in mmol/mol. The modern *Operculina*
808 *ammonides* data represents the average value of five globally-spaced samples reported in (Evans
809 et al., 2013). See Table 1 for Mg/Ca data.

Figure 1

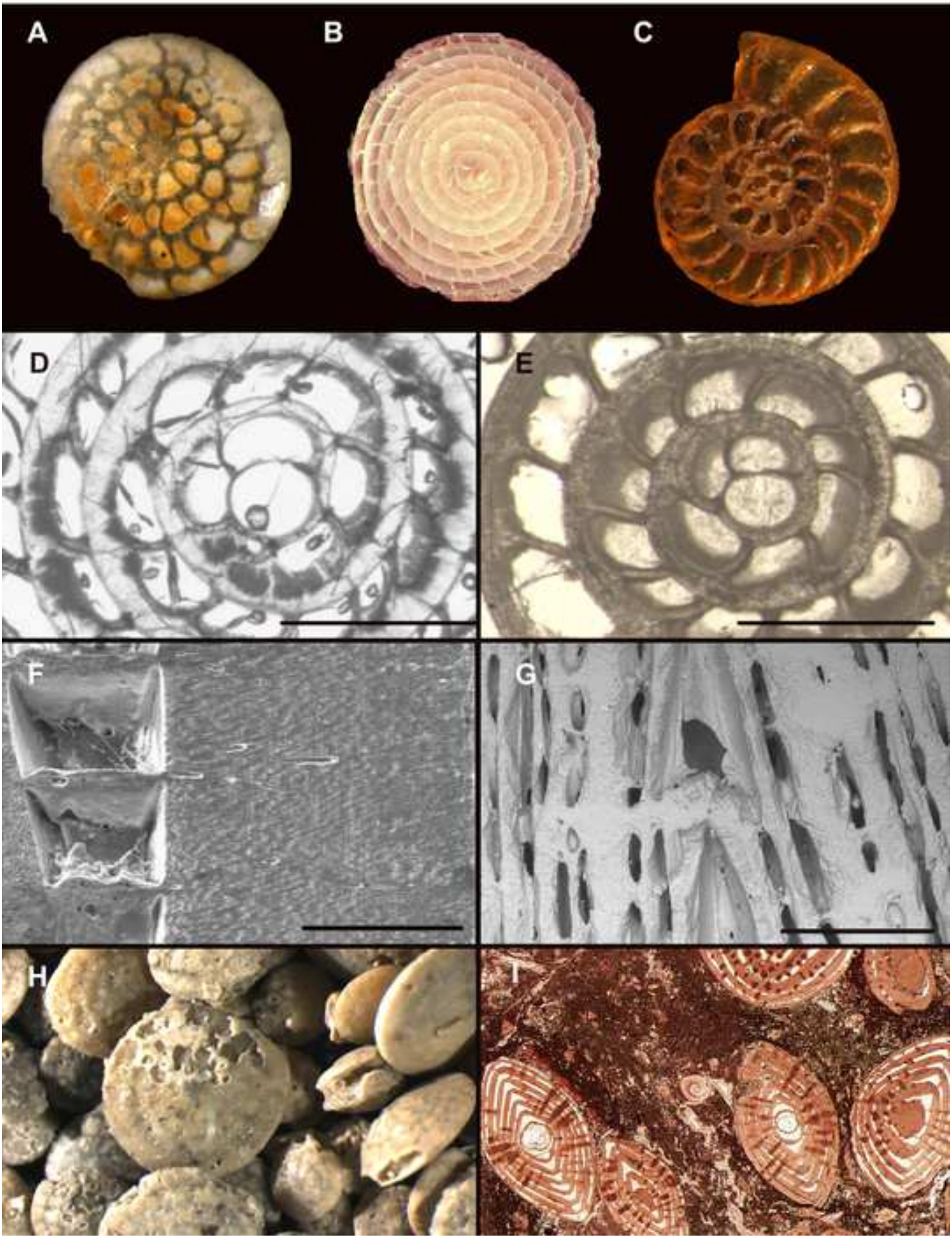

Figure 2

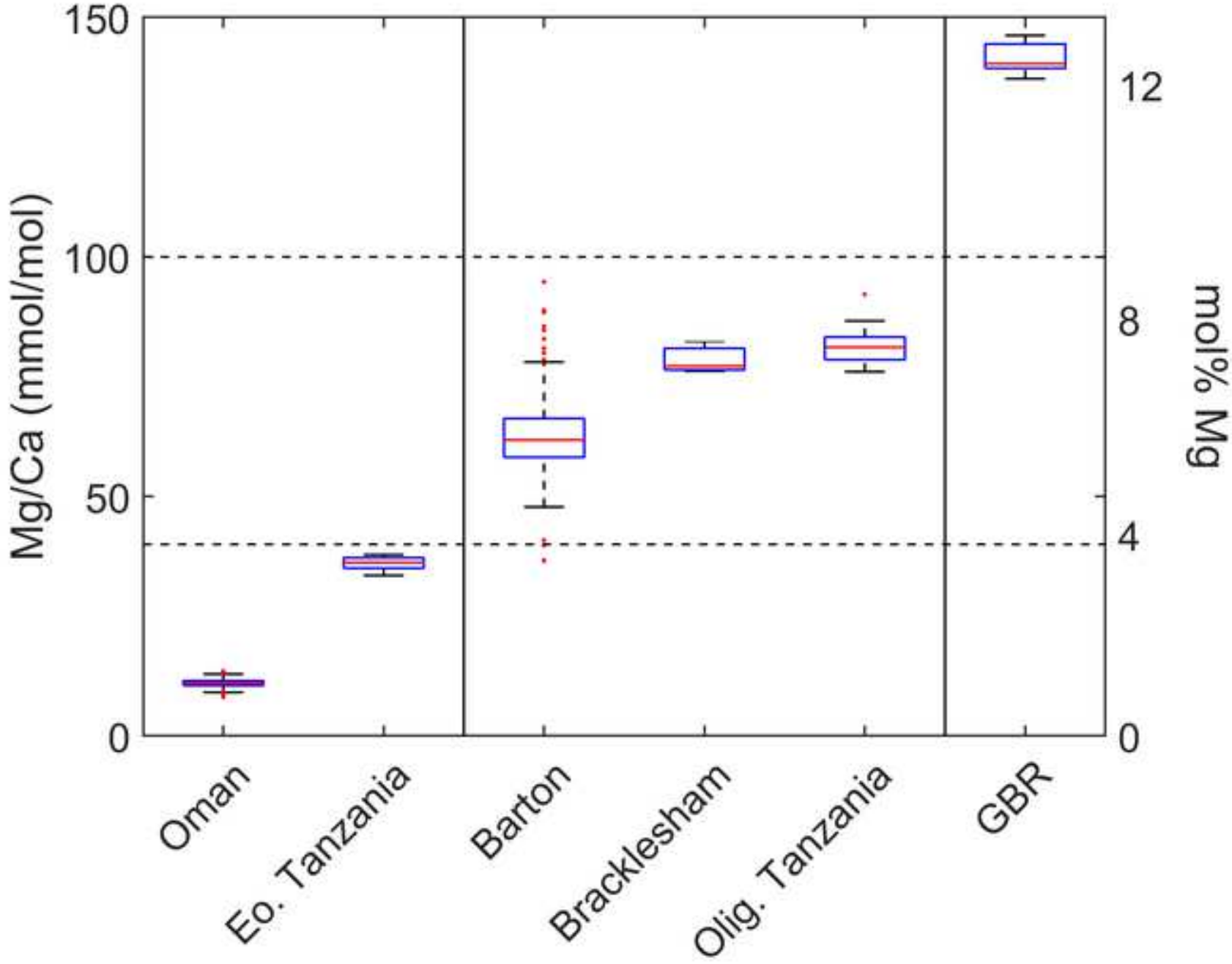
150
100
50
0
Mg/Ca (mmol/mol)
12
8
4
0
mol% Mg
Oman
Eo. Tanzania
Barton
Bracklesham
Olig. Tanzania
GBR

Figure 3

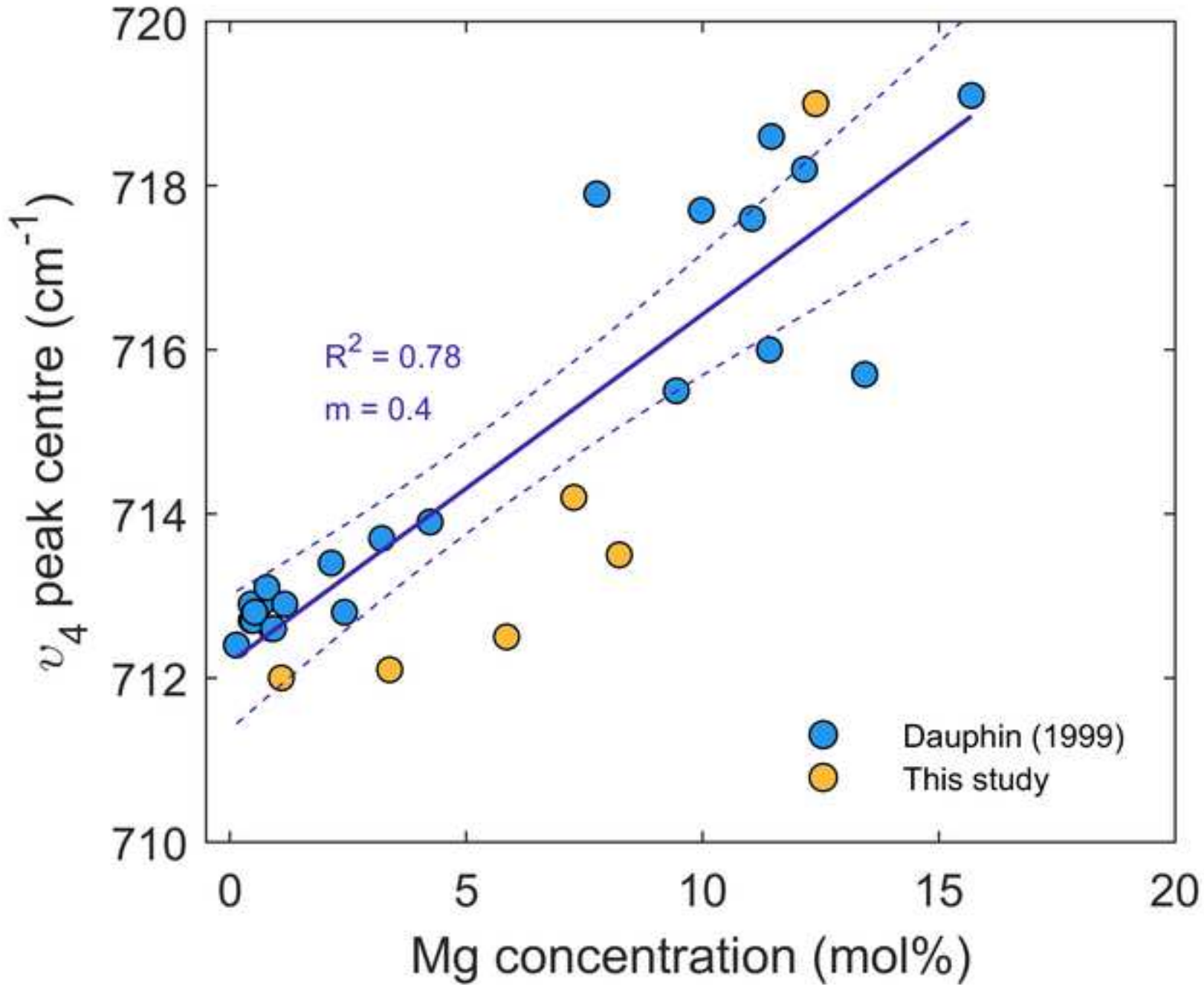
720
718
716
714
712
710
0
5
10
15
20
υ_4 peak centre (cm^{-1})
Mg concentration (mol%)
R^2 = 0.78
m = 0.4
Dauphin (1999)
This study

Figure 4

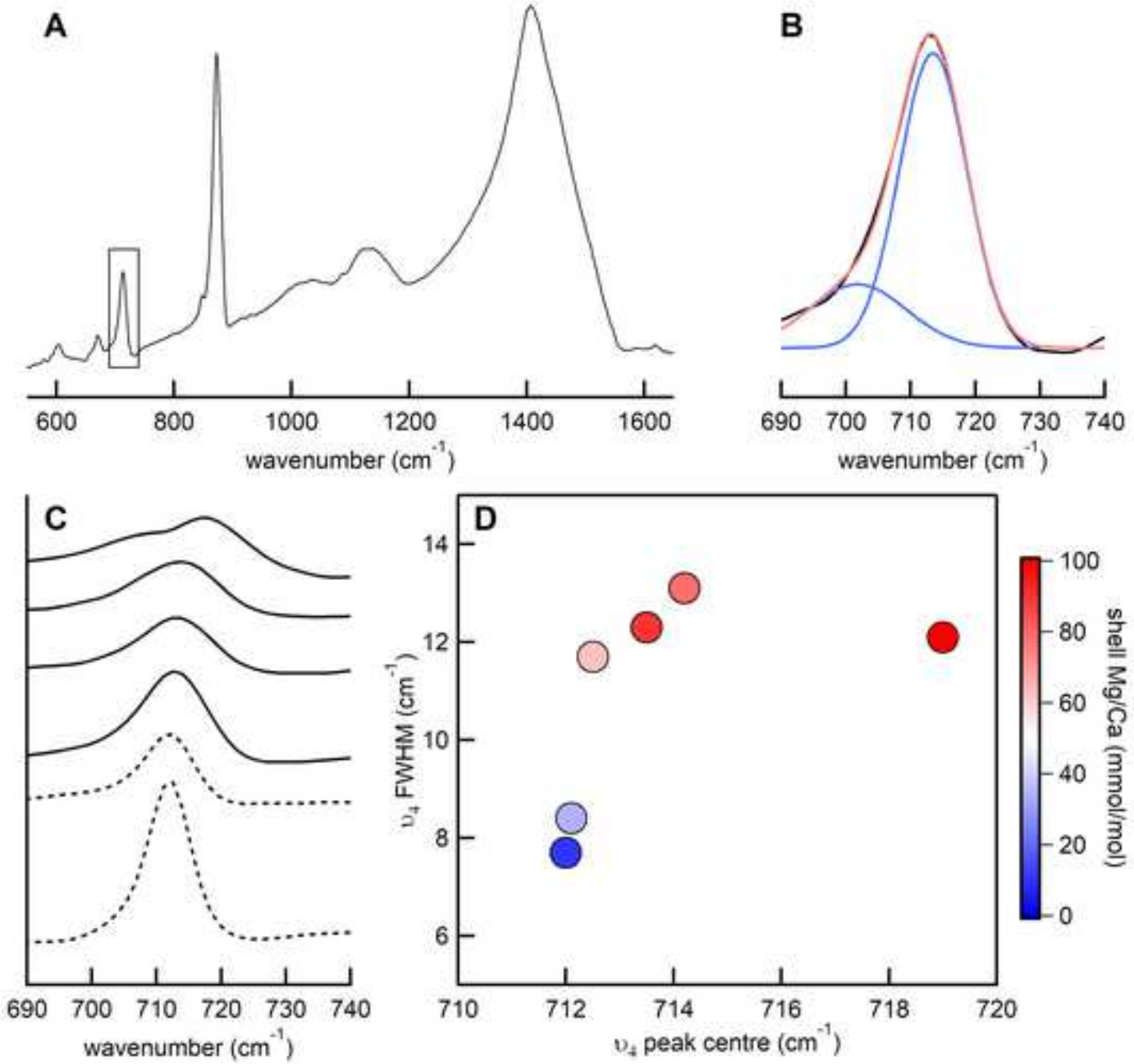
A
600
800
1000
1200
1400
1600
wavenumber (cm-1)
B
690
700
710
720
730
740
wavenumber (cm-1)
C
690
700
710
720
730
740
wavenumber (cm-1)
D
14
12
10
8
6
υ4 FWHM (cm-1)
710
712
714
716
718
720
υ4 peak centre (cm-1)
100
80
60
40
20
0
shell Mg/Ca (mmol/mol)

Figure 5

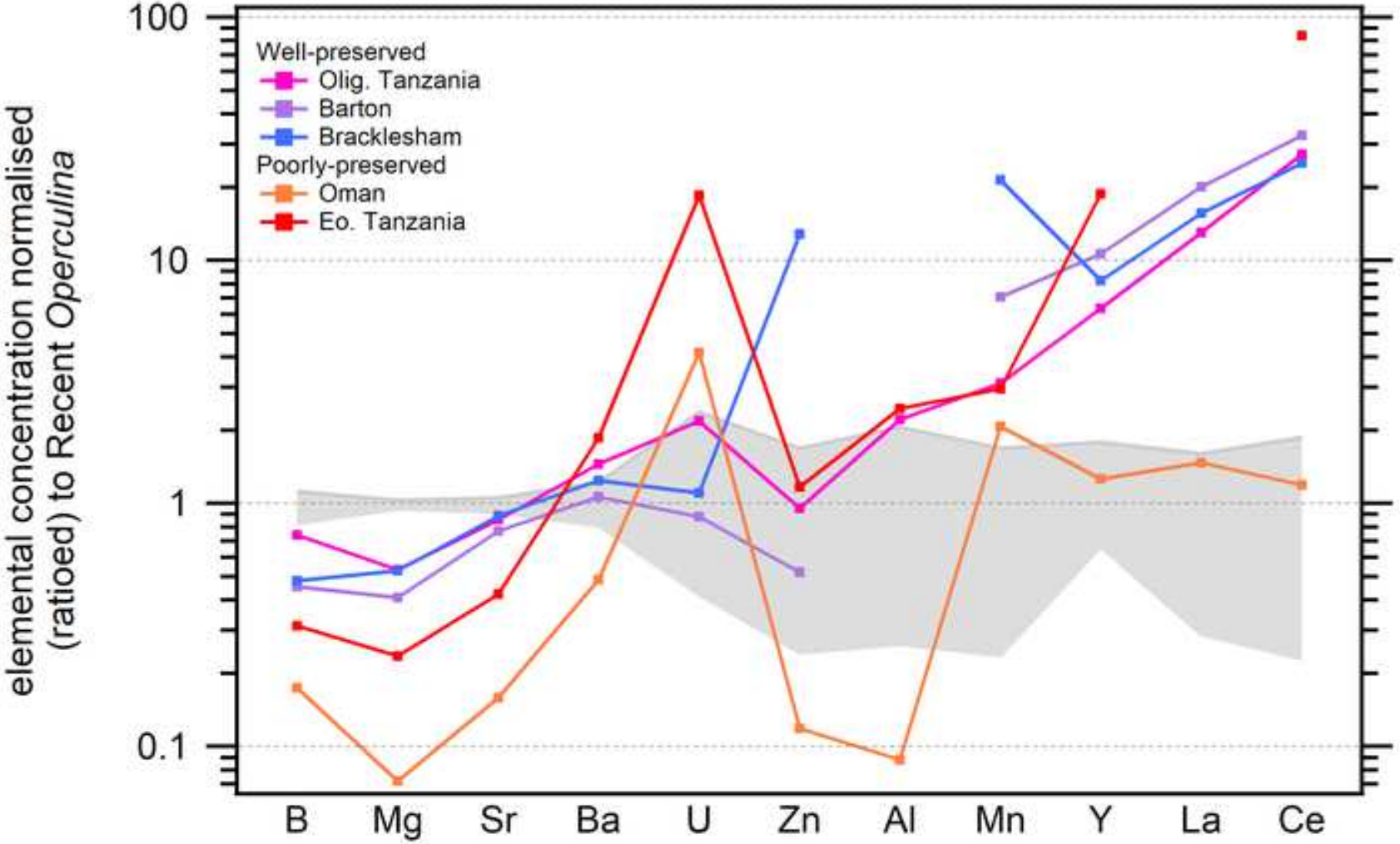
100
10
1
0.1
elemental concentration normalised
(ratioed) to Recent Operculina
Well-preserved
Olig. Tanzania
Barton
Bracklesham
Poorly-preserved
Oman
Eo. Tanzania
B
Mg
Sr
Ba
U
Zn
Al
Mn
Y
La
Ce

Table 1

Locality	Taxa	Age	Visual preservation	LA-ICPMS Mg/Ca (mmol/mol†)	XRD Mg/Ca (mol%)	υ_4 position (cm^{-1})	υ_4 FWHM (cm^{-1})
GBR Australia	*Operculina ammonoides*	Modern	N/A	141.5 (12.4)	-	719.0‡	12.1
Japan	*Cycloclypeus carpenteri*	Modern	N/A	-	12.8	-	-
Tanzania	*Nummulites* ssp	EOT (earliest Oligocene)	Exceptional	89.8 (8.2)	6.0	713.5	12.3
Tanzania	Echinoid fragment	EOT	Exceptional	-	6.0	713.0	13.2
Bracklesham/ Whitecliff Bay	*Nummulites laevigatus*	Middle Eocene	Exceptional	78.5 (7.28)	6.0	714.2	13.1
Alum bay (Barton Fm)	*Nummulites prestwichianus*	Bartonian	Exceptional	60.9 (5.7)	6.0	712.5	11.7
Tanzania	*Nummulites* ssp	EOT (latest Eocene)	Poor/average	35.0 (3.4)	0	712.1	8.4
Oman	*Nummulites*	Eocene	Poor/average	11.0 (1.09)	0	712.0	7.7

†mol% given in parentheses

‡This sample has a pronounced split υ_4 peak (the other is located at 708.1 cm^{-1}, see Fig. 4C)

Table 2

Sample	B/Ca	Al/Ca	Mn/Ca	Zn/Ca	Sr/Ca	Y/Ca	Ba/Ca	La/Ca	Ce/Ca	U/Ca
Modern *Operculina*	354	118	18.1	5.4	2.40	0.53	2.79	0.13	0.21	0.06
Olig. Tanzania	262	260	56.4	5.2	2.06	3.4	4.06	1.7	5.6	0.13
Alum Bay	161	n.d.	127.5	2.8	1.85	5.6	2.97	2.7	6.8	0.05
Bracklesham	170	n.d.	386.5	69.1	2.14	4.4	3.47	2.1	5.2	0.07
Oman	62	10	37.4	0.64	0.38	0.67	1.35	0.20	0.25	0.25
Eo. Tanzania	111	288	53.5	6.3	1.02	10.0	5.20	n.d.	17.3	1.1